Separation Science and Technology
Publication details, including instructions for authors and subscription information:
http://www.informaworld.com/smpp/title~content=t713708471

A Wastewater Treatment System Applying Aeration-Cavitation Flotation Mechanism

M. Nonaka[a]
[a] Department of Mineral Development Engineering, The University of Tokyo, Tokyo, Japan

To cite this Article Nonaka, M.(1986) 'A Wastewater Treatment System Applying Aeration-Cavitation Flotation Mechanism', Separation Science and Technology, 21: 5, 457 — 474
To link to this Article: DOI: 10.1080/01496398608056129
URL: http://dx.doi.org/10.1080/01496398608056129

SEPARATION SCIENCE AND TECHNOLOGY, 21(5), pp.457-474, 1986

A Wastewater Treatment System Applying Aeration-Cavitation Flotation Mechanism

M. NONAKA

DEPARTMENT OF MINERAL DEVELOPMENT ENGINEERING
THE UNIVERSITY OF TOKYO
TOKYO 113, JAPAN

Abstract

A new type of wastewater treatment system applying not only aeration but also the cavitation flotation mechanism is proposed to attain high capacity and low operation cost. The system can be operated continuously in a single or multistage with ease. The system is composed of four isolated sections: feed section, aeration section, multiphase flow section, and separation section. Aeration and gas dissolution are carried out in the aeration section. Then collisions between the elements to be removed and gas bubbles, and cavitation of dissolved gas are accomplished in the multiphase flow section, followed by the recovery of the aggregates as the froth product in the separation section. The function of each section is evaluated by taking into consideration the contribution to the separation characteristics. It is confirmed through a series of treatment tests that the separation rate is a few tens of times faster than those in conventional treatment systems and, hence, lower energy consumption is anticipated in the proposed system.

INTRODUCTION

Development of an effective wastewater treatment technique is essential for the preservation of the environment. A wastewater treatment process operated with high capacity and low cost is urgently needed, especially for industries where enormous quantities of water are consumed. Most wastewater treatment systems employ chemical or biological techniques, but many have poor capacities.

Flotation techniques have recently been applied to several wastewater treatment processes (*1-7*). Elements to be removed are ions, colloids, and/

 0149-6395/86/2105-0457$3.50/0

or fine solid particles in the aqueous phase. Hence, an enormous number of finely dispersed gas bubbles has to be generated in the flotation cell. Dissolved gas flotation techniques have been developed to meet this requirement, but the separation rates have been too slow to increase the capacity. Moreover, continuous operations are not easily achieved in conventional dissolved gas flotation systems.

To cope with these problems, a new type of wastewater treatment system applying not only aeration but also the cavitation flotation mechanism has been developed. The system is composed of the four isolated sections: feed section, aeration section, multiphase flow section, and separation section. In this paper the function of each section is evaluated, taking into consideration the pressure loss or the collision rate of the elements to be removed with gas bubbles. Moreover, the results obtained from experimental work carried out with wastewater containing heavy metal ions or fine solid particles in a single and multistage system are discussed from the separation kinetics and energy consumption viewpoints.

GENERAL VIEW OF THE SYSTEM

The system is illustrated conceptually in Fig. 1. The feed section is composed of a head tank and a feed pipe. Wastewater conditioned with chemicals is fed into the head tank in batch or continuous operation, and it flows down the feed pipe. A head tank-feed pipe system can be substituted for a sump-pump system. The head tank-feed pipe system is preferable in continuous multistage operation.

Pressured wastewater is fed into the aeration section (referred to as an aerator). The aerator utilizes a cyclone action, i.e., wastewater is tangentially fed into the cyclone-like part of the aerator and produces a spray discharge from the outlet. If compressed air or a specific gas is needed, it is introduced through a nozzle placed at the center of the cyclone-like part of the aerator. The air or gas is dispersed into an enormous number of fine gas bubbles due to the shear stress generated by the spray flow, while a small part of the gas is dissolved in the liquid phase of the wastewater.

Baffle plates placed on the bottom of the aerator serve to prevent the coalescence of gas bubbles due to the swirling flow. Moreover, the baffle plates enhance turbulence, and the turbulent shear stress serves to disperse more minute gas bubbles. In the aerator a small amount of the elements to be removed attach to the gas bubbles. A detail drawing of the aerator is shown in Fig. 2.

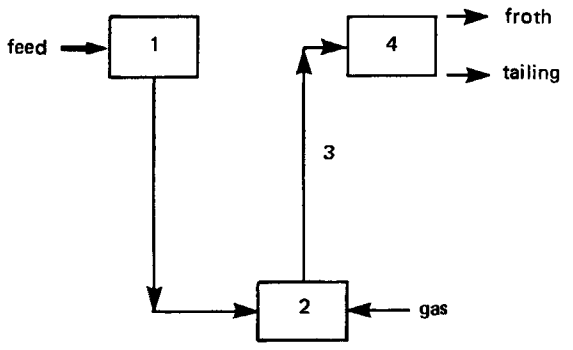

FIG. 1. Conceptual illustration of the system: (1) feed section, (2) aeration section, (3) multiphase flow section, (4) separation section.

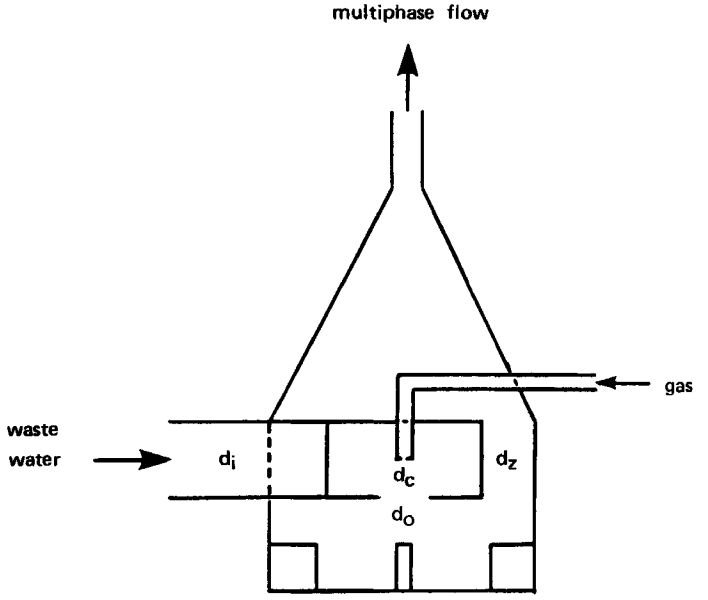

FIG. 2. Configuration of the aerator.

The aerated wastewater flows upward in a vertical pipe in which a stable multiphase bubble flow is established. The pipe is referred to as a gas-lift pipe. In the pipe the attachment of elements to be removed to gas bubbles is promoted by collisions due to turbulent mixing. Moreover, dissolved gas in the aerator cavitates as extremely minute gas bubbles in the gas-lift pipe when the flow goes upward and pressure is released. Dissolved gas tends to nucleate, preferentially on the hydrophobic surfaces of the elements contained in wastewater (*8*).

The upper end of the gas-lift pipe is connected with the separation section (referred to as a separator). Then the aggregates of gas bubbles with elements which have to be removed are separated by buoyancy in the separator. The aggregates are floated from the liquid phase in a gravity force field if the attached elements are easily detached from gas bubbles. The separation of the elements attached to fine gas bubbles is enhanced in a centrifugal force field. Thus the utilization of centrifugal force, which is easily attained by the application of a cyclone mechanism, should increase the separation rate and hence the capacity of the system.

In a multistage operation the effluent from the separator, or the tailing, in the first treatment stage is fed into the head tank in the following stage. The multistage operation is essential for increasing the capacity and the separation efficiency of the treatment system. Moreover, the multistage operation can be continuously controlled by a single pump and a single compressor.

The scale of the system is determined by the throughput. Roughly speaking, the throughput is proportional to the square root of the effective head pressure, which can be substituted for the effective height of the head tank. Thus, the height of the head tank measured from the aerator inlet level was 2–3 m in a laboratory test and about 10 m in a pilot test.

FUNCTION OF EACH SECTION

Feed Section

The pressure balance of the system in the steady state is written as

$$P_{FH} - P_{FL} - P_{AL} - P_{MH} - P_{ML} - P_{SH} - P_{SL} = 0 \qquad (1)$$

where P_{FH} is the hydrostatic pressure in the feed section, P_{FL} is the pressure loss in the feed pipe, P_{AL} is the pressure loss in the aerator, P_{MH} is

the hydrostatic pressure in the multiphase flow section, P_{ML} is the pressure loss in the gas-lift pipe, P_{SH} is the hydrostatic pressure in the separation section, and P_{SL} is the pressure loss in the separator. The hydrostatic pressure in the separator is inconsequential compared with the other terms. Thus the function of the feed section is to supply the principal driving force ($P_{FH} - P_{FL}$) to the system. The pressure loss in the feed pipe can be approximately determined by formulas describing the friction losses in the straight pipe flow and the bend flow of the continuous phase because the volume fraction of the dispersed phase is extremely small in conventional wastewater.

Aeration Section

One of the most important factors in the system is to generate stable gas bubbles. The generation of gas bubbles in the aerator is principally due to the shear force induced by the spray discharge from the outlet orifice of the cyclone-like part. A gas body is formed in the water wall of the spray flow when gas is introduced, and it is dispersed as fine bubbles at the interface between the spray flow and the bulk of the liquid phase. Thus the bubble size is determined by the force balance between the shear stress and the capillary pressure of the gas bubbles. Hence, the bubble diameter is given by

$$d_b = 4\sigma_{w/g}/S \tag{2}$$

where $\sigma_{w/g}$ is the liquid-gas interfacial tension and S is the shear stress on the interface. The higher the aeration rate, the larger the dispersed gas bubbles, but a few very large bubbles are generated at a critical aeration rate due to insufficient shear stress. The critical value is called the maximum aeration rate, which is defined as the ratio of the maximum gas flow rate to the sum of the liquid and gas flow rates.

The maximum aeration rate was observed by using a separate aerator whose orifice diameter was varied. The cyclone-like part of the aerator had a diameter of 40 mm. Tap water containing frother (ACC-Aerofroth No. 65) was directly fed into the aerator by a centrifugal pump. The frother concentration was 15 mg/L. Effects of the flow rate and orifice diameter on the maximum aeration rate are shown in Fig. 3. Thus it has been confirmed that the aeration rate in this system is much higher than in conventional flotation systems which have an aeration rate of 0.2 at the highest (*9*). Moreover, it has been proved by experiments carried out in a single-stage continuous system of laboratory scale that the maximum aeration rate at the separator inlet level reaches about 0.5.

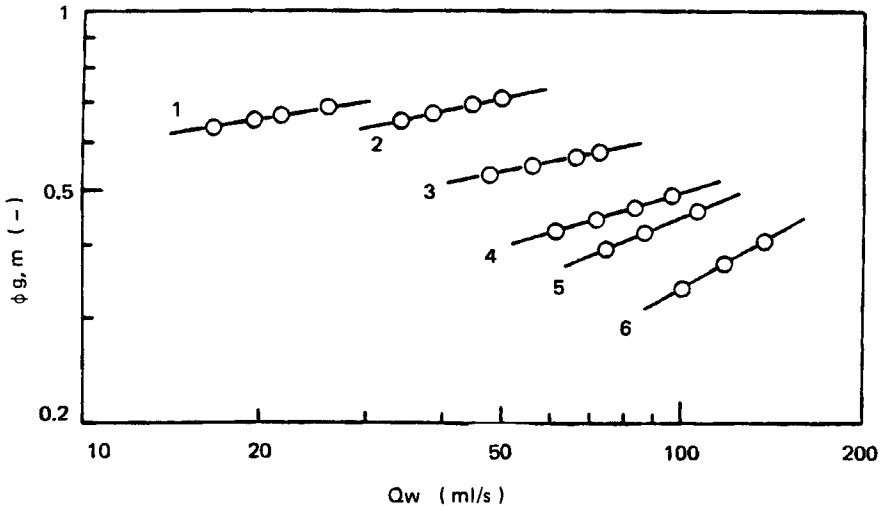

FIG. 3. Effect of the flow rate Q_w on the maximum aeration rate ϕ_{gm} (d_c = 40 mm). d_o = 2 mm (1), 3 mm (2), 4 mm (3), 5 mm (4), 6 mm (5), 8 mm (6).

The maximum aeration rate should be determined by the tangential and axial velocities of the liquid phase flowing through the orifice of the cyclone-like part of the aerator. The tangential velocity has a decisive effect on the maximum aeration rate:

$$v_{t,o} = a \cdot v_i(d_c/d_o)^n = a \cdot 4Q_w/(\pi d_i^2)(d_c/d_o)^n \quad (3)$$

where $v_{t,o}$ is the tangential velocity at the orifice, v_i is the inlet velocity, d_c is the diameter of the cyclone-like part of the aerator, d_o is the orifice diameter, d_i is the inlet diameter, Q_w is the flow rate of wastewater, and a and n are constants determined from the geometrical configuration of the aerator and the physical properties of wastewater. The maximum gas flow rate through the orifice is Q_{gm}, and hence the apparent axial gas velocity, $v_{g,z} = 4Q_{gm}/(\pi d_0^2)$ is correlated with the tangential velocity. The effect of the tangential velocity of the liquid phase on the maximum apparent velocity of the gas phase through the orifice is shown in Fig. 4, which has been calculated from Fig. 3 by introducing $a = n = 0.8$. These values for a and n were derived from measurement of the tangential velocity profile in the cyclone-like part of the aerator. As can be seen, the maximum gas velocity

is correlated with the tangential velocity by a power law, the coefficient of which is determined by the dimensions of the cyclone-like part of the aerator.

Another function of the aerator is to disperse additional gas bubbles through the action of the baffle plate due to turbulent shear. Applying Kolmogoroff's theory to the dispersion phenomena, the turbulent shear stress S_t is represented as

$$S_t \propto \rho_w(\varepsilon d_b)^{2/3} \tag{4}$$

where ρ_w is the density of wastewater and ε is the dissipation energy of turbulence per unit time and unit mass. Taking into consideration the capillary pressure of a bubble equilibrated with the shear stress, the stable bubble diameter is

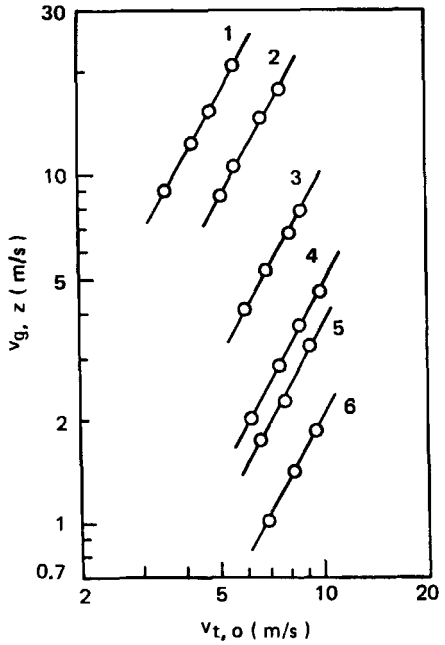

FIG. 4. Effect of the tangential velocity of liquid phase at the orifice $v_{t,o}$ on the apparent axial velocity of the gas phase through the orifice of the aerator v_{gz} (d_c = 40 mm). d_o = 2 mm (1), 3 mm (2), 4 mm (3), 5 mm (4), 6 mm (5), 8 mm (6).

$$d_b \propto (\sigma_{w/g}/\rho_w)^{3/5}\varepsilon^{-2/5} \tag{5}$$

Thus, turbulent shear stress is utilized for the dispersion or the prevention of bubble coalescence. Dissolution of the gas phase into the aqueous phase is an additional function of the aerator. The dissolution process is not an equilibrium state because residence time in the aerator is extremely short. Hence, the mass of dissolved gas in the aqueous phase of wastewater must be less than that predicted from Henry's law.

Pressure loss in the aerator is mainly governed by the pressure loss in the cyclone-like part. The pressure loss was observed in various types of aerators, and the results were submitted to dimensional analysis. One of the significant dimensionless terms is the pressure loss factor, defined by

$$\xi = 2P_{AL}/(\rho_w v_i^2) \tag{6}$$

and another is the aerator Reynolds number, given by

$$\mathrm{Re}_a = \rho_w v_i d_c/\mu_w \tag{7}$$

where μ_w is the viscosity of the wastewater. The relationship between these two terms is illustrated in Fig. 5. Considering that the Reynolds number in practical operation may be above 10^5, the pressure loss factor does not depend on the Reynolds number but on the size ratio of the aerator. Then effects of d_i/d_c, d_o/d_c, and d_z/d_c on the pressure loss were evaluated experimentally. As a result, d_z/d_c was confirmed to have little effect on the pressure loss, while the other two ratios had significant effects. Thus the pressure loss has been correlated with the flow rate and the dimensions of the cyclone-like part of the aerator by

$$Q_w = Kd_i d_o (d_c/d_o)^{1-m}(2P_{AL}/\rho_w)^{1/2} \tag{8}$$

where the dimensionless constant K and m are 0.2 and 0.8, respectively, when the spray discharge from the orifice is uniform. However, they show larger values when the spray discharge is segregated.

Multiphase Flow Section

Collisions between the elements to be removed and dispersed and the cavitated gas bubbles are mainly governed by turbulent mixing in the

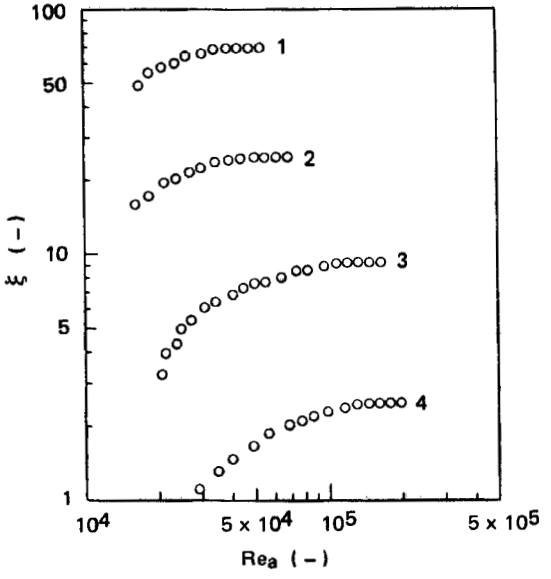

FIG. 5. Dependence of the pressure loss factor ξ on the aerator Reynolds number Re_a. $d_o/d_c = 0.1$ (1), 0.15 (2), 0.25 (3), 0.5 (4).

gas-lift pipe. The turbulent characteristics in the pipe were observed by using the electrode reaction technique (*10*). The Eulerian time correlation function of the fluctuating velocities of the liquid phase is defined by

$$R_E(\tau) = \overline{u'(t) \cdot u'(t+\tau)} \,/\, \overline{u'^2} \tag{9}$$

where u' is the fluctuating velocity, and t and τ are times. The Eulerian time correlation function observed in the axial direction is shown in Fig. 6. As can be seen, the Eulerian correlation function is approximated by

$$R_E(\tau) = \exp\{-\pi\tau^2/(4T_E^2)\} \tag{10}$$

where T_E is the Eulerian integral time scale given by

$$T_E = \int_0^\infty R_E(\tau)d\tau \tag{11}$$

The integral time scale decreased when the Reynolds number in the gas-lift pipe was increased.

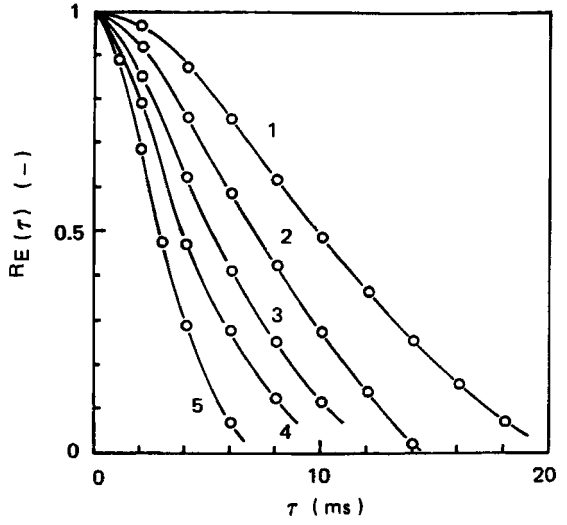

FIG. 6. Eulerian time correlation function $R_E(\tau)$ in the gas-lift pipe ($\phi_g = 0.2$). Re = 7.58×10^3 (1), 1.01×10^4 (2), 1.52×10^4 (3), 1.77×10^4 (4), 2.02×10^4 (5).

Moreover, assuming isotropy of turbulence, one can calculate the dissipation energy per unit time and unit mass in the gas-lift pipe by

$$\varepsilon = 15\pi\nu\overline{u'^2}/\Lambda_f^2 \tag{12}$$

where ν is the kinematic viscosity and Λ_f is the integral space scale of the longitudinal velocity correlation function (*11*). The integral space scale can be approximated by

$$\Lambda_f = \bar{u} \cdot T_E \tag{13}$$

where $\bar{u}$ is the mean velocity. Thus the dissipation energy of turbulence in the axial direction has been confirmed to be of the order of 10^{-3} m^2/s^3 in the gas lift-pipe.

It has also been deduced from Eq. (10) that the turbulent energy in the gas-lift pipe is propagated by diffusive mixing (*12*). Thus the collision process can be regarded as a diffusion process of the elements to be removed against the gas bubbles. The diffusion process of the elements to a single gas bubble is written as

$$\frac{\partial C}{\partial t} = \frac{1}{r^2}\left(\frac{\partial}{\partial r}\right)\left(r^2 D_t \frac{\partial C}{\partial r}\right) \tag{14}$$

in the spherical coordinate system, where C is the concentration on a count basis of the elements per unit volume, D_t is the turbulent diffusion coefficient, and r is the space coordinate. Substituting the diffusion coefficient for Kolmogoroff's diffusion coefficients (*13*) given by

$$D_t = \alpha(\varepsilon r)^{1/3} \cdot r; \qquad r \geqslant \lambda_0 \tag{15}$$

$$= \beta(\varepsilon/\nu)^{1/2} \cdot r^2; \qquad r < \lambda_0 \tag{16}$$

Eq. (14) can be solved analytically in the steady state under the boundary conditions

$$\left.\begin{aligned} r = R; \qquad & C = 0 \\ r = \infty; \qquad & C = C_0 \end{aligned}\right\} \tag{17}$$

where α and β are constants, R is the collision radius, while λ_0 is Kolmogoroff's microscale given by

$$\lambda_0 = (\nu^3/\varepsilon)^{1/4} \tag{18}$$

In the gas-lift pipe the microscale has been confirmed to be of the order of 10^{-1} mm.

The number of collisions of the elements per unit time with a single gas bubble, or the collision rate process, is

$$-\frac{dC_0}{dt} = 4\pi R^2 \cdot \left(D_t \frac{\partial C}{\partial r}\right)_{r=R} \tag{19}$$

Taking into consideration the continuity at $r = \lambda_0$ and that the bubble diameter is larger than $2\lambda_0$, the overall collision rate in reference to aerated gas bubbles is given by

$$-dC_0/dt = (28\pi\alpha/3)R^{7/3} \cdot \varepsilon^{1/3} \cdot n_{b,a} \cdot C_0 \tag{20}$$

where $n_{b,a}$ is the number of aerated gas bubbles per unit volume. Assuming that the bubble diameter is constant and much larger than the

element diameter, the collision process in a given gas-lift pipe can be rewritten

$$-dC_0/dt = K_a \cdot \phi_g \cdot \varepsilon^{1/3} \cdot C_0 \tag{21}$$

On the other hand, the collision process in reference to cavitated gas bubbles, if allowable, is described by

$$-dC_0/dt = K_c \cdot \varepsilon^{1/2} \cdot n_{b,c} \cdot C_0 \tag{22}$$

because the collision radius may be smaller than Kolmogoroff's microscale, where $n_{b,c}$ is the number of cavitated gas bubbles per unit volume. The collision process may not, however, be realizable because the dissolved gas preferentially nucleates on the hydrophobic surfaces of the elements.

Thus the dissipation energy, and hence the intensity of turbulence in the gas-lift pipe, can be regarded as a determinant of the separation kinetics of the system. Another function of the gas-lift pipe is to decrease the backpressure to the aerator, which is promoted by increasing the gas hold-up. It is, however, accompanied by an increased pressure loss because the flow velocity of the liquid phase becomes faster in a higher gas hold-up state.

Separation Section

The elements attached to gas bubbles are recovered in the separation section. Therefore, the separation rate is also a determinant of system performance. Centrifugal force, applied through a cyclone-like separation mechanism, is used to recover the gas bubbles. The shear force of the cyclone-like separator has to be controlled so it will not detach the elements from the gas bubbles. Assuming that the behavior of the gas bubbles in the centrifugal field is dominated by Stokes' law and that the tangential velocity in the separator is given by a power law such as Eq. (3), the time necessary for the gas phase in the separator feed to be transferred to the separating zone of the cylindrical cyclone-like separator is

$$t_s = (9\pi/16)(\mu_w/Q)(d_i^2/d_b^2)\{d_s^2/(a - a \cdot n)\}\{1 - (d_f/d_s)^{2-2n}\} \tag{23}$$

where Q is the total flow rate into the separator, d_i is the inlet diameter, d_s is the diameter of the cylindrical separator, d_f is the diameter of the separating zone in which gas bubbles are recovered as the froth product,

and d_b is the bubble diameter, while a and n are constants involved in the power law describing the tangential velocity profile in the separator. The mean residence time of the feed in the separator is given by

$$t_m = (\pi/4)(d_s^2/Q)\{1 - (d_f/d_s)^2\} \cdot h_s \tag{24}$$

where h_s is the height of the cylindrical separator. Hence, macroscopically, gas bubbles are recovered when $t_m > t_s$.

The tangential velocity in the separator should not be as fast as the velocity in the hydrocyclone used for solid classification because the aggregates of the elements with gas bubbles have a small mass and are apt to collapse. Hence, the pressure loss in the separator is negligible compared with the pressure losses in other sections, as proven experimentally.

EXPERIMENTAL

As a model of the wastewaters containing heavy metal ions or solid particles, deionized water containing copper ions, designated as "wastewater I," and deionized water containing fine quartz particles, designated as "wastewater II," were prepared. In order to prepare wastewater I, reagent grade copper sulfate was dissolved in deionized water to obtain a solution of 20 mg-Cu/L. Copper ions precipitate as copper sulfide when a solution is sufficiently aerated. For the preparation of wastewater II, fine quartz particles (−50 μm) were suspended in deionized water to establish a concentration of 20 mg/L.

Collectors used for wastewater I and wastewater II were anionic potassium ethyl xanthate and cationic dodecyl ammonium chloride, respectively. The concentrations of both chemicals were fixed at 10^{-4} mol/L. Water-soluble frother (ACC-Aerofroth No. 65) was also added to each wastewater. The wastewaters, after being conditioned for a definite time at a regulated pH, were subjected to treatment tests. The units in the treatment system had the following dimensions:

Level of the head tank	2.5 m
Diameter of the feed pipe	20 mm
Diameter of the cyclone-like part of the aerator	40 mm
Diameter of the orifice of the aerator	4 mm
Diameter of the gas-lift pipe	20 mm
Level of the separator	2.5 m

Diameter of the cylindrical cyclone-like separator	75 mm
Height of the cylindrical part of the separator	150 mm

The aeration rate observed at the inlet level of the separator was about 0.5 for both wastewaters. The flow rate, or the throughput of the system, was about 180 mL/s. The tailing, or residue, from the separator in the first stage was also treated in the second stage. Wastewater I and wastewater II were treated in three-stage systems in this manner.

The flotation rate behaviors are illustrated in Fig. 7. Nonfloat Y is defined by

$$Y = (eE)/(fF) \tag{25}$$

where e and f are the concentrations of solids or metal ions in the tailing of each stage and the raw wastewater, respectively, while E and F are the flow rates of the tailing of each stage and the feed into the system. Flotation time is calculated from the mean residence time in the gas-lift pipe and the separator. Assuming that the flotation behavior in the

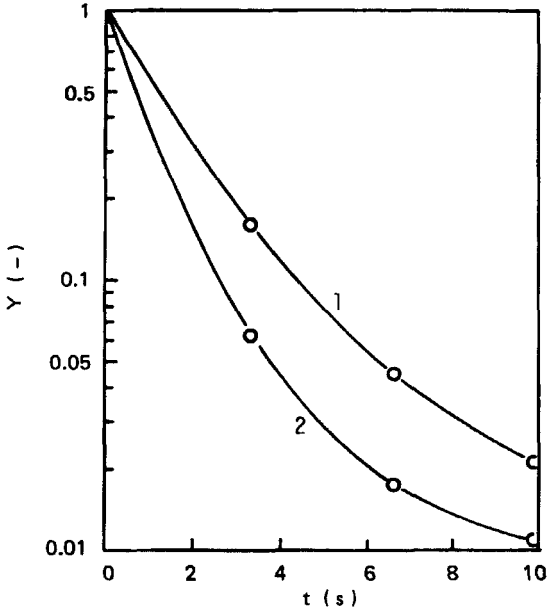

FIG. 7. Variation of nonfloat Y with flotation time t for wastewater I (1) and wastewater II (2).

system is mainly governed by collisions of the elements with gas bubbles in the gas-lift pipe, the flotation process is macroscopically regarded as a first-order rate process as can be seen from Eq. (21). The flotation behavior as a rate process is written as

$$Y = \exp(-kt) \tag{26}$$

where k is called the flotation rate constant (*14, 15*). Thus the flotation rate constants have been quantified as 33.3 min^{-1} for wastewater I and 50.6 min^{-1} for wastewater II in the first stage. As can be seen from Fig. 7 the flotation rate in the second and third treatment stages is slower than that predicted from Eq. (26), which must be caused by dilution of the reagents, detachment of the attached elements from gas bubbles, and degradation of the collected elements.

Thus it has been confirmed that the flotation rate constant in the proposed wastewater treatment system is a few tens of times greater than that in a mechanical flotation system in which the rate constant is less than 1 min^{-1} (*16*). Hence, the throughput of the proposed system will be a few tens of times greater than that of the conventional system having the same effective volume. In order to gain the identical throughput, the effective volume of a conventional treatment system has to be enlarged a few tenfolds, which means that a large number of flotation cells are needed in a conventional flotation system. This would increase both maintenance and running costs. On the other hand, control of the proposed multistage treatment system requires only a pump, which serves to supply raw wastewater to the head tank in the first stage, and a compressor, which determines the aeration rate or the flow rate. Therefore, lower energy consumption is anticipated for the proposed wastewater treatment system compared with conventional mechanical flotation systems.

CONCLUSION

A new type of wastewater treatment system employing not only an aeration but also a cavitation flotation mechanism has been proposed for the treatment of wastewater containing various kinds of ions and/or suspended solids. The system is composed of four isolated sections: feed section, aeration section, multistage flow section, and separation section. The function of each section has been evaluated by taking into consideration the contribution to the separation phenomena. The aeration rate in the aerator can be increased up above 0.5, so that the

possibility of contact of the elements with gas bubbles is enhanced remarkably compared with conventional flotation systems. The attachment of elements to gas bubbles is dominated by diffusive mixing in the gas-lift pipe where cavitated minute gas bubbles also play an important role. Moreover, the separation rate is increased by utilizing a cyclone-like separator. The overall separation rate, and hence the capacity of the system, has proven to be a few tens of times larger than those in conventional wastewater treatment systems through a series of multistage treatment tests.

SYMBOLS

a	constant involved in Eq. (3)
C	concentration on count basis (m^{-3})
C_0	concentration on count basis at r = (m^{-3})
D_t	turbulent diffusion coefficient (m^2/s)
d_b	bubble diameter (mm)
d_c	diameter of the cyclone-like part of the aerator (mm)
d_f	diameter of the separating zone in the separator (mm)
d_i	inlet diameter (mm)
d_o	orifice diameter (mm)
d_s	diameter of the cylindrical cyclone-like separator (mm)
d_z	height of the cyclone-like part of the aerator (mm)
E	flow rate of the tailing in each stage (mL/s)
e	concentration of the tailing in each stage (mg/L)
F	flow rate of the feed into the system (mL/s)
f	concentration of the feed (mg/L)
h_s	height of the separator (mm)
K	constant involved in Eq. (8)
K_a	constant involved in Eq. (21)
K_c	constant involved in Eq. (22)
k	flotation rate constant (min^{-1})
m	constant involved in Eq. (8)
n	constant involved in Eq. (3)
$n_{b,a}$	number of aerated gas bubbles per unit volume (m^{-3})
$n_{b,c}$	number of cavitated gas bubbles per unit volume (m^{-3})
P_{AL}	pressure loss in the aeration section (Pa)
P_{FH}	hydrostatic pressure in the feed section (Pa)
P_{FL}	pressure loss in the feed section (Pa)

P_{MH} hydrostatic pressure in the multiphase flow section (Pa)
P_{ML} pressure loss in the multiphase flow section (Pa)
P_{SH} hydrostatic pressure in the separation section (Pa)
P_{SL} pressure loss in the separation section (Pa)
Q total flow rate (mL/s)
Q_{gm} maximum gas flow rate (mL/s)
Q_w flow rate of wastewater (mL/s)
R collision radius (mm)
$R_E(\tau)$ Eulerian time correlation function (—)
Re_a aerator Reynolds number (—)
r space coordinate
S shear stress involved in Eq. (2) (N/m^2)
S_t turbulent shear stress (N/m^2)
t time (s)
t_m mean residence time in the separator (s)
t_s time defined by Eq. (23) (s)
$\bar{u}$ mean velocity (m/s)
u' fluctuating velocity (m/s)
v_i inlet velocity (m/s)
v_{gz} axial gas velocity (m/s)
$v_{t,o}$ tangential velocity at the orifice of the aerator (m/s)
Y nonfloat (—)

Greek

α constant involved in Eq. (15)
β constant involved in Eq. (16)
ε dissipation energy of turbulence (m^2/s^3)
Λ_f integral space scale of the longitudinal velocity correlation function (mm)
λ_0 Kolmogoroff's microscale (mm)
μ_w viscosity of wastewater (Pa · s)
ν kinematic viscosity (m^2/s)
ξ pressure loss factor (—)
ρ_w density of wastewater (kg/m^3)
$\sigma_{w/g}$ liquid–gas interfacial tension (N/m)
T_E Eulerian integral time scale (ms)
τ time (ms)
ϕ_g aeration rate (—)

Acknowledgments

The author wishes to thank Professor T. Inoue of the Department of Mineral Development Engineering, The University of Tokyo, for instructive discussions, and Mr H. Ohta, former assistant in the Department for valuable contributions to the experimental work, and Mr S. Tabata, chemical analyst in the Department, for his chemical analyses effort on the treatment products.

REFERENCES

1. A. Bahr, *Erzmetall, 30*, 572 (1977).
2. J. L. Steiner, G. F. Bennett, E. F. Mohler, and L. T. Clere, *Chem. Eng. Prog., 74*, 39 (1978).
3. D. Raicevic, *CIM Bull., 72*, 109 (1979).
4. N. D. Sylvester and J. J. Byeseda, *Soc. Pet. Eng. J., 20*, 579 (1980).
5. R. A. Conway, R. F. Nelson, and B. A. Young, *J. Water Pollut. Control Fed., 53*, 1198 (1981).
6. J. R. Bratby, *Ibid., 54*, 1558 (1982).
7. W. T. Shannon, W. R. Owers, and H. P. Rothbaum, *Geothermics, 11*, 43 (1982).
8. V. I. Klassen and V. A. Mokrousov, in *An Introduction of the Theory of Flotation*, Butterworth, London, 1963, Section II.
9. C. C. Harris, in *Flotation: A. M. Gaudin Memorial Volume*, Vol. 2, AIMMPE, New York, 1976, Chap. 27.
10. T. Mizushina, *Heat Transfer, 7*, 87 (1971).
11. J. O. Hinze, in *Turbulence*, 2nd ed., McGraw-Hill, New York, 1975, p. 56.
12. M. Nonaka, T. Inoue, and T. Imaizumi, in *The 14th International Mineral Processing Congress*, Vol. 3, Toronto, 1982, p. 9.1.
13. V. G. Levich, in *Physicochemical Hydrodynamics*, Prentice-Hall, Englewood Cliffs, New Jersey, 1962, p. 215.
14. T. Imaizumi and T. Inoue, in *Proceedings of the 6th International Mineral Processing Congress* (A. Roberts, ed.), Pergamon, Oxford, 1965, p. 581.
15. T. Inoue and T. Imaizumi, in *Preprints of the 8th International Mineral Processing Congress*, Leningrad, 1968, S-15.
16. T. Imaizumi, T. Inoue, M. Nonaka, and Y. Minemura, in *Special Project Research on Detection and Control of Environmental Pollution*, Vol. 3, 1979, p. 123.

Received by editor July 29, 1985